

CONTROL OF LASER RADIATION PARAMETERS https://doi.org/10.1070/QEL16407

Specific features of oscillation regimes of an external cavity diode laser under microwave modulation

A.A. Isakova, K.N. Savinov, N.N. Golovin, N.Zh. Altynbekov, V.I. Vishnyakov, A.K. Dmitriev

Abstract. **Under microwave modulation of the pump current of a diode laser (λ = 795 nm), an oscillating dependence of the amplitudes of side components of the emission spectrum on frequency is observed. The relation of these oscillations with the field structure in a laser cavity and with the optical thickness of the cavity diffraction grating is found.**

Keywords: *rubidium frequency standard, diode laser, microwave pumping.*

1. Introduction

Research aimed to increase the stability of quantum frequency standards has been continuously performed since the creation of masers and lasers [1]. Narrow spectral resonances both in optical and microwave ranges are used as references in quantum frequency standards. The uncertainty of the best frequency standards reaches $\sim 10^{-16}$ [2, 3].

For the last decades, a caesium standard has been chosen as the primary standard possessing the frequency of 9.192 GHz. All microwave standards (hydrogen or based on alkaline earth atoms) employ forbidden transitions between hyperfine structure sublevels of the ground state.

Combining two ground states with a common excited state through two coherent radiations at frequencies matching two allowed optical transitions leads to interference effects during excitation. If the frequency difference between the light waves matches the clock frequency, a fluorescence dip is observed. This phenomenon predicted in [4] is termed coherent population trapping (CPT). Actually, at the same time, CPT-resonances were detected in a cell with sodium atoms [5]. One of the main applications of the CPT-resonances is their employment as references in frequency standards [6]. There are also reported applications in magnetometry [7, 8], induced transparency [9–11], atom cooling [12] and precision spectroscopy [13].

A.A. Isakova, K.N. Savinov, N.N. Golovin, N.Zh. Altynbekov
Novosibirsk State Technical University, prosp. Karla Marksa 20, 630073 Novosibirsk, Russia; e-mail: alina100@mail.ru;
V.I. Vishnyakov Institute of Laser Physics, Siberian Branch, Russian Academy of Sciences, prosp. Akad. Lavrent'eva 13/3, 630090 Novosibirsk, Russia; e-mail: split7fire@yandex.ru;
A.K. Dmitriev Novosibirsk State Technical University, prosp. Karla Marksa 20, 630073 Novosibirsk, Russia; Institute of Laser Physics, Siberian Branch, Russian Academy of Sciences, prosp. Akad. Lavrent'eva 13/3, 630090 Novosibirsk, Russia;
e-mail: alexander_dmitriev@ngs.ru

Received 20 April 2017
Kvantovaya Elektronika **47** (7) 610–613 (2017)
Translated by N.A. Raspopov

The most popular now is a rubidium clock, the first samples of which employed a spectral lamp filled with rubidium vapours as a source of optical pumping [14]. It was shown [15] that the minimal shifts are specific of the hyperfine transition $5S_{1/2}(F=2)-5S_{1/2}(F=1)$ of the ground state of the D_1-line of isotope rubidium-87 at a wavelength of 795 nm. Differences in the widths and amplitudes of CPT-resonances of the absorption lines D_1 and D_2 are related to different structures of the magnetic sublevels of the excited P-state. Comparison of CPT-resonance parameters for Rb atoms has shown that the employment of the D_1-line provides an approximately 10 times greater intensity of the CPT-resonances than the D_2-line can provide.

Presently, rubidium clocks are often pumped by vertical cavity lasers, which have an advantage of low energy consumption and small size [16, 17]. This allows one to modulate the emission spectrum of this laser efficiently in a wide range of ultra-high frequencies including the clock transition frequency.

Optical pumping of CPT-resonances in rubidium atoms by a single laser was realised under sinusoidal modulation of the injection current in an AlGaAs laser diode at a wavelength of 780 nm [18]. Under the sub-harmonic frequency modulation at a frequency of 1.139 GHz with a modulation index of 4.2, a resonance with a width of 3 kHz was detected at a clock frequency of 6.834682613 GHz.

In addition, efficient microwave pumping of a diode laser was demonstrated at a higher frequency, where the latter coincided with the mode separation value of the laser cavity [19]. However, the problem of accuracy needed for matching the laser cavity length with the modulation frequency was still open.

In this work, we present investigation results on the efficiency of microwave pumping of an external cavity diode laser at a wavelength of 795 nm versus the modulation frequency near the resonance value.

2. Experimental setup

An ECDL-7940RF diode laser (S/N 061332 Vita Wave) was used in the work. An optical scheme of the diode laser is shown in Fig. 1. One face of the laser diode (*1*) had an AR-coating. The laser radiation passed to an aspheric lens (*2*), then, the light beam of aperture δ passed to a diffraction grating (*3*). The latter was installed in such a way that the cavity length provided the value of the laser mode separation near half the frequency of the clock transition $5S_{1/2}(F=2)-5S_{1/2}(F=1)$ of the ground state for the D_1-line of isotope rubidium-87. The optical thickness of the grating (and the corresponding uncertainty of the cavity length Δl) is related to the light beam diameter δ by the relationship: $\Delta l = \delta \operatorname{tg}\alpha$, where α is the angle of light beam incidence to the grating. Since in our case the diffraction grating (1800 lines mm^{-1}) was

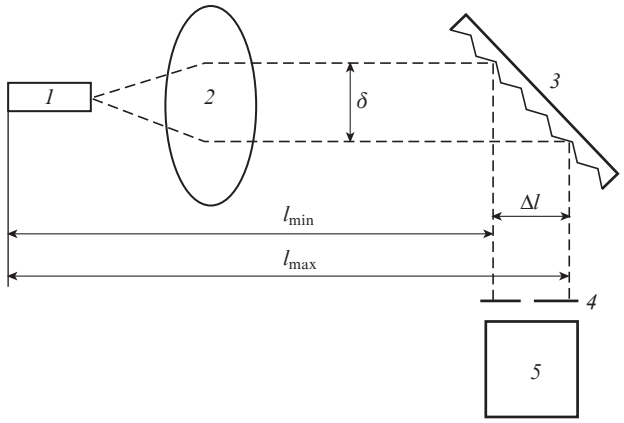

Figure 1. Optical scheme of a diode laser:
(*1*) laser diode; (*2*) aspheric lens; (*3*) diffraction grating; (*4*) diaphragm; (*5*) photodetector; δ is the width of the light beam; l_{max} and l_{min} are the maximal and minimal possible lengths of the laser cavity, respectively; $\Delta l = l_{max} - l_{min}$ is the optical thickness of the diffraction grating (the laser cavity length uncertainty).

installed at an angle close to 45° the optical thickness of the grating was actually determined by the aperture of the light beam, i.e., $\Delta l = \delta$.

A scheme for measuring a laser emission spectrum is presented in Fig. 2. Signals from a DC power supply (*1*) and from a microwave oscillator (*3*) passed through a ZFBT-6GW-FT mixer (*2*) to a diode laser (*4*). The laser light was directed through an optical isolator (*5*) to a Fabry–Perot interferometer (*6*) formed by plane mirrors with transmissions of 5% and 40% for the input and output mirrors, respectively. The output mirror was mounted on a piezoceramic transducer (*7*), which provided scanning a distance between the interferometer mirrors by means of a digital tooth voltage generator (*9*). The light that had passed through the interferometer was detected by a photodetector (*8*), a signal from which was fed to a digital oscilloscope (*10*). A signal from the tooth voltage generator passed to the second channel of the oscilloscope for matching scans with the interferometer wavelength (frequency).

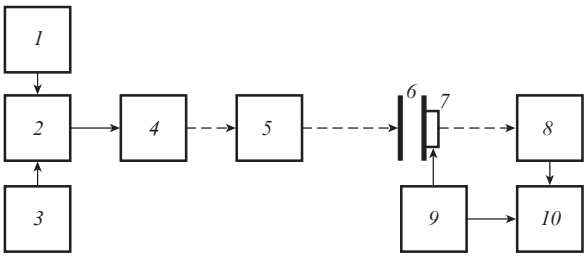

Figure 2. Scheme for measuring laser emission spectrum:
(*1*) laser power supply; (*2*) mixer; (*3*) microwave-oscillator; (*4*) diode laser; (*5*) optical isolator; (*6*) Fabry–Perot interferometer; (*7*) piezoceramic transducer; (*8*) photodetector; (*9*) tooth voltage generator; (*10*) digital oscilloscope.

3. Experimental results and discussion

Spectral measurements were performed at a wavelength of 795 nm for a laser pump current of 72 mA and a microwave oscillator signal of 16 dBm. Without modulation, the laser operated in a single-mode regime with the emission linewidth of $\sim 10^4$ Hz. The free spectral range of the Fabry–Perot interferometer was 20 GHz, and the tooth voltage scanning time was 0.1 s. The maximal value of the side component amplitudes was observed at a frequency $f_0 = 3.54$ GHz (Fig. 3). The intensities of the central and side components were normalised to the intensity of the signal corresponding to the absence of modulation. Because the resonance modulation frequency f_0 is related to the cavity optical length l by the relationship $f_0 = c/2l_0$, where c is the speed of light, the effective laser cavity length l_0 corresponding to this frequency is 42 mm. The amplitude of the high-frequency component was lower than that of the low-frequency one. Seemingly, this is related to the fact that, in addition to the frequency modulation, there was amplitude modulation as well.

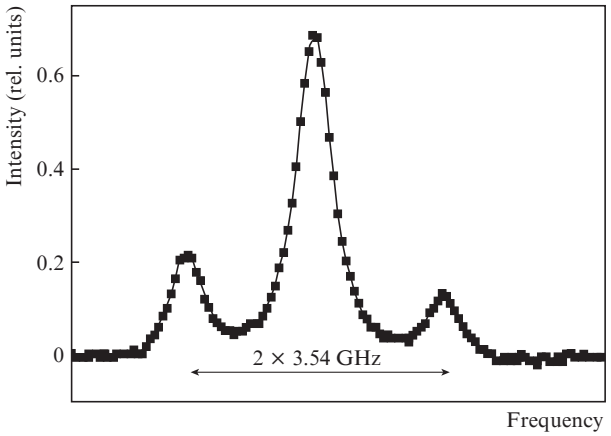

Figure 3. Spectrum of laser radiation at the pump frequency $f_0 = 3.54$ GHz.

Reliability of experimental data was increased by making ten measurements of the amplitude dependences of side components on the microwave-oscillator frequency. These dependences were of oscillating character (Fig. 4). The microwave-oscillator frequency f varied with a step of 0.01 GHz. The interval between neighbouring maxima was $\sim$0.08 GHz, and the FWHM width of the main lobe near the frequency $f_0 =$ 3.54 GHz was 0.15 GHz. The amplitude of the low-frequency component was greater than of the high-frequency compo-

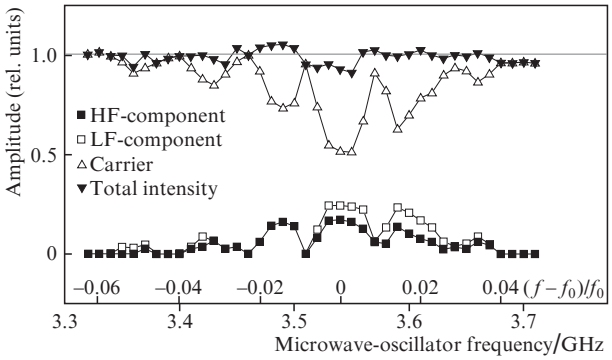

Figure 4. Amplitudes of side components, carrier and total intensities vs. modulation frequency.

nent over the entire frequency range. Minimal amplitudes of the carrier corresponded to maxima of the side components. As expected, the sum intensity of the side spectral components and the carrier was equal to the intensity of non-modulated laser radiation within the measurement error. The frequency range comprising observed side components was $\Delta f = 0.3 \pm 0.03$ GHz, and the relative width was $\Delta f/f_0 = 0.085 \pm 0.01$.

For determining the optical thickness of the diffraction grating and clarifying a reason of amplitude oscillations of the side spectral components in laser radiation versus the modulation frequency we have measured distributions of laser radiation intensity (see Fig. 1) by a photodetector with a diaphragm of diameter 0.206 mm attached to it. The photodetector was placed on a two-coordinate stage controlled by step motors. Distributions of light beam intensities at various distances from the diffraction grating were recorded with a step of 0.2 mm along both the horisontal (x) and vertical (y) coordinates (Fig. 5). For each distance, 10 measurements were made and after statistical treatment the cross-section profiles were obtained with a standard deviation.

At the output from the laser (Fig. 5a), the distribution of the radiation intensity has a close-to-elliptical shape; the distributions in the horisontal and vertical planes (cross sections) are almost Gaussian. The width of the light beam in the horizontal plane and, correspondingly, the optical thickness of the diffraction grating was $\sim 3.3 \pm 0.3$ mm, which yields the ratio $\Delta l/l_0 = 0.08 \pm 0.008$. This value coincides with the width given above for the frequency range, in which the side components were observed, $\Delta f/f_0 = 0.085 \pm 0.01$. Hence, one may assert that the range of effective modulation ultra-high frequencies is determined by the optical thickness of the diffraction grating.

However, a smooth distribution of the radiation intensity at the laser output does not explain reasons of observed oscil-

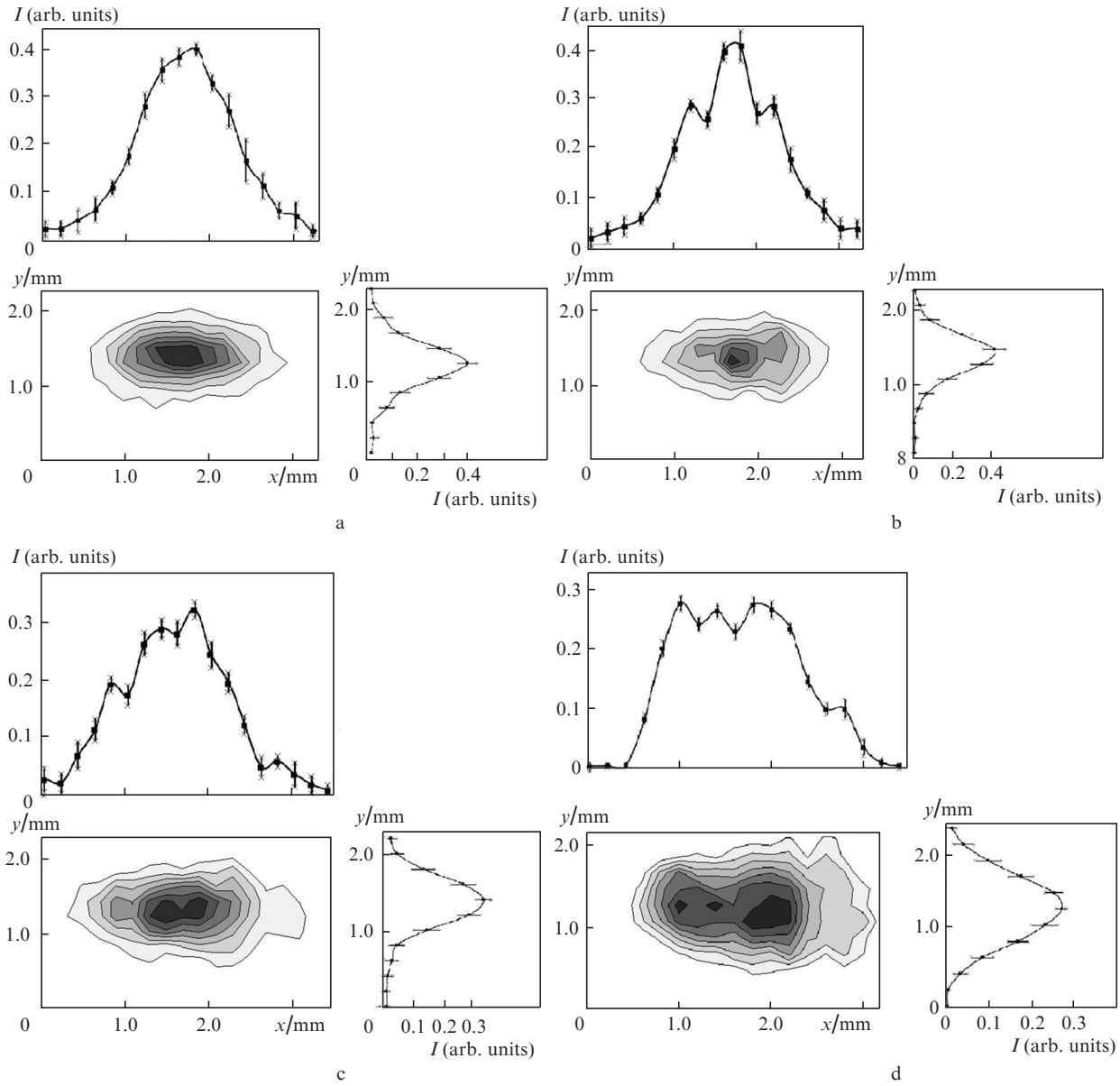

Figure 5. Cross-section laser radiation intensity distributions at distances from the diffraction gratings: (a) 12), (b) 211, (c) 428 and (d) 898 mm. A greater value along the x axis corresponds to a longer cavity. While plotting topograms, the intensity was divided to eight zones from zero to the maximal levels. Black colour corresponds to the maximal level.

lations (Fig. 4). In order to clarify the nature of these oscillations, we investigated profiles of laser intensity distributions at various distances from the diffraction grating. At a greater distance, the horizontal profile of the radiation intensity distribution becomes fragmented. At a distance of 898 mm from the diffraction grating (Fig. 5d), the cross-section profile is qualitatively similar to the dependence of side component amplitudes on the modulation frequency (Fig. 4). Note that a lower frequency corresponds to a greater length. Fragmentation of the cross-section profiles is related to the structural character (oscillating dependence) that the wavefront acquires in the horizontal plane on the diffraction grating of the laser cavity. The structure, in turn, may be related to a complicated combined cavity and defects of the diffraction grating.

Thus, an oscillating amplitude dependence of the side components on the microwave signal frequency has been observed. Seemingly, this dependence can be explained by the employment of a complicated combined laser cavity. The frequency range, in which the side components are observed, was 0.3 GHz, and the FWHM width of the main lobe near the frequency f_0 = 3.54 GHz was 0.15 GHz. This means that for efficient modulation at a frequency near half that of the clock transition (3.42 GHz) the effective laser cavity length should be 44 mm with the relative error of at most 0.04.

Acknowledgements. This work was supported by the Ministry of Education and Science of the Russian Federation (Grant No. 3.6835.2017/8.9) in the frameworks of the base part of the government research task and by the Russian Foundation for Basic Researches (Grant No. 15-02-02557).

References

1. Quinn T. (Ed). *Metrologia*, **42** (3), S1–S153 (2005).
2. Bize S., Laurent P., Abgrall M., Marion H., Maksimovic I., Cacciapuoti L., Grunert J., Vian C., Pereira dos Santos F., Rosenbusch P., Lemonde P., Santarelli G., Wolf P., Clairon A., Luiten A., Tobar M., Salomon C. *J. Phys. B: At. Mol. Opt. Phys.*, **38**, 449 (2005).
3. Hollberg L., Oates C.W., Wilpers G., Hoyt C.W., Barber Z.W., Diddams S.A., Oskay W.H., Bergquist J.C. *J. Phys. B: At. Mol. Opt. Phys.*, **38**, 469 (2005).
4. Arimondo E., Orriols G. *Lettere Al Nuovo Cimento*, **17**, 333 (1976).
5. Alzetta G., Gozzini A., Moi M., Orriols G. *Il Nuovo Cimento*, **36**, 5 (1976).
6. Vanier J. *Appl. Phys. B*, **81**, 421 (2005).
7. Scully O., Fleischhauer M. *Phys. Rev. Lett.*, **69**, 1360 (1992).
8. Nagel A., Graf L., Naumov A., Mariotti E., Biancalana V., Meschede D., Wynands R. *Europhys. Lett.*, **44**, 31 (1998).
9. Harris E. *Phys. Today*, **50**, 36 (1997).
10. Kasapi A., Jain M., Yin G.Y., Harris S.E. *Phys. Rev. Lett.*, **74**, 2447 (1995).
11. Scully M.O., Zubairy M.S. *Quantum Opt.*, **67**, 648 (1999).
12. Aspect A., Arimondo E., Kaiser R., Vansteenkiste N., Cohen-Tannoudji C. *J. Opt. Soc. Am. B*, **6**, 2112 (1989).
13. Wynands R., Nagel A. *Appl. Phys. B*, **68**, 1 (1999).
14. Bell W.E., Bloom A.L. *Phys. Rev. Lett.*, **6**, 280 (1961).
15. Stähler M., Wynands R., Knappe S., Kitching J., Hollberg L., Taichenachev A., Yudin V. *Opt. Lett.*, **27**, 1472 (2002).
16. Vanier J., Levine M., Kendig S., Janssen D., Everson C., Delaney M., in *Proc. IEEE Int. Ultrasonics, Ferroelectrics, Frequency Control Joint 50th Anniversary Conf.* (New York: IEEE, 2004) p. 92.
17. Khripunov S.A., Radnatarov D.A., Kobtsev S.M., Yudin V.I., Taichenachev A.V., Basalaev M.Yu., et al. *Quantum Electron.*, **46**, 668 (2016) [*Kvantovaya Elektron.*, **46**, 668 (2016)].
18. Cyr N., Têtu M., Breton M. *IEEE Trans. Instrum. Meas.*, **42**, 640 (1993).
19. Bagayev S.N., Volkov V.G., Ivashko D.Yu., Matyugin Yu.A., Fateev N.V. *Quantum Electron.*, **29**, 109 (1999) [*Kvantovaya Elektron.*, **26**, 109 (1999)].